Published in final edited form as:
Chem Biol Drug Des. 2006 October ; 68(4): 183–193. doi:10.1111/j.1747-0285.2006.00432.x.

Cell Signaling and Trafficking of Human Melanocortin Receptors in Real Time Using Two-photon Fluorescence and Confocal Laser Microscopy: Differentiation of Agonists and Antagonists

Minying Cai[1], **Eva V. Varga**[2], **Magda Stankova**[1], **Alexander Mayorov**[1], **Joseph W. Perry**[1,3], **Henry I. Yamamura**[2], **Dev Trivedi**[1], and **Victor J. Hruby**[1,*]

1 *Department of Chemistry, University of Arizona, Tucson, AZ 85721, USA*

2 *Department of Pharmacology, University of Arizona, Tucson, AZ 85721, USA*

3 *Department of Chemistry & Biochemistry, Georgia Institute of Technology, Atlanta, GA 30332, USA*

Abstract

Melanocortin hormones and neurotransmitters regulate a vast array of physiologic processes by interacting with five G-protein-coupled melanocortin receptor types. In the present study, we have systematically studied the regulation of individual human melanocortin receptor wild subtypes using a synthetic rhodamine-labeled human melanotropin agonist and antagonist, arrestins fused to green fluorescent protein in conjunction with two-photon fluorescence laser scanning microscopy and confocal microscopy. Stimulation of the melanocortin receptors by its cognate agonist triggered rapid arrestin recruitment and receptor internalization for all four human melanocortin receptors examined. Antagonists-bound melanocortin receptors, on the other hand, did not recruit *β*-arrestins, and remained in the cell membrane even after long-term (30 min) treatment. Agonist-mediated internalization of all melanocortin receptor subtypes was sensitive to inhibitors of clathrin-dependent endocytosis, but not to caveolae inhibitors. In summary, agonist-mediated internalization of all subtypes of melanocortin receptors are dependent upon *β*-arrestin-mediated clathrin-coated pits, whereas, *β*-arrestin-2 conjugated green fluorescence protein (*β*-arrestin-2-GFP) recruitment is not dependent on protein kinase A activation. Real time two-photon fluorescence laser scanning microscopy is a most powerful tool to study the dynamic processes in living cells and tissues, without inflicting significant and often lethal damage to the specimen.

Keywords

β-arrestin; green fluorescence protein; melanocortin receptors; MTII; rhodamine; SHU-9119; two-photon fluorescence laser scanning microscopy

Membrane proteins are highly interesting drug targets as many of them serve as receptors, and are involved in intercellular communication and in control of intracellular functions critical for many aspects of health and disease. The melanocortin system consists of melanotropin peptides derived from the pro-opiomelanocortin (POMC) gene, five melanocortin receptors, two endogenous antagonists and two ancillary proteins (1). Recent pharmacologic and genetic studies have affirmed the role of melanocortins in pigmentation (1), inflammation (2), immune response (3,4), blood pressure and heart rate (5), energy homeostasis (6–8), feeding behavior and sexual dysfunction (7–11), and other bioactivities (1). Development of receptor selective

*Corresponding author: Victor J. Hruby, hruby@u.arizona.edu.

agonists and antagonists will further facilitate the investigation of these complex physiologic functions and provide an experimental basis for new pharmacotherapies (12).

The human melanocortin-1 (*h*MC1) receptor is mainly expressed in melanocytes and leukocytes and has been implicated in the regulation of the immune system, inflammatory responses, and skin pigmentation (13–15). The *h*MC2 receptor, on the other hand, is expressed in the adrenal cortex and mediates glucocorticoneogenesis (16). The native hormone for this receptor is ACTH and will not be further considered in this study. The *h*MC3 and *h*MC4 receptors are mainly present in the central nervous system (17), but their distribution patterns are different (17). The *h*MC3 and *h*MC4 receptors are thought to play complementary roles in weight control (18,19). Finally, the hMC5 receptor is found in a variety of peripheral tissues and plays an important role in the regulation of exocrine gland function (20). These discoveries have intensified the interest in melanocortin receptor pharmacology. For example, design of highly selective and potent hMC4 receptor agonists is expected to provide efficient pharmacotherapeutics for the treatment of obesity (7,21,22).

Much effort has been made both in industry and academia to develop melanocortin drugs, especially for the treatment of obesity and erectile function, and for effects on pigmentation. The use of melanocortin receptor agonists in clinical practice; however, may encounter potential problems due to the rapid reduction of the pharmacologic effects upon longer-term treatment by agonists for the *h*MCRs inducing desensitization, internalization, and downregulation. Receptor desensitization, internalization, and downregulation are common and predictable phenomena caused by most GPCR agonists (23). Presently, however, very little is known about the molecular mechanisms of all subtypes melanocortin receptors regarding internalization, desensitization, and downregulation which are of critical importance to understand the potential drug response mediated by agonists that might lead to the rational selective drug design.

In a recent communication (24), we reported on the use of two-photon fluorescence laser scanning microscopy (TPFLSM) to observe internalization of hMCRs activated by melanotropin agonists versus antagonists. In order to address the possibility that different *h*MCR subtypes follow differential internalization and/or desensitization pathways which might be able to shed useful information for selective drug design, we have performed further detailed comparisons of the internalization mechanisms of the four human melanocortin receptors (*h*MCR1, *h*MCR3, *h*MCR4, *h*MCR5) which use α-MSH as its ligand, by using fluorescent-labeled (rhodamine, -Rho) derivatives of the non-selective melanocortin agonist MTII (Ac-Nle-c[Asp-His-D-Phe-Arg-Trp-Lys]-NH_2, Ac-Nle-c[Asp^5, D-Phe^7, Lys^{10}] α-MSH (4–10)-NH_2) (25), (Rho-MTII), and of the hMC3 and hMC4 receptor antagonist SHU-9119 (Ac-Nle-c[Asp-His-D-Nal(2′)-Arg-Trp-Lys]-NH_2, Ac-Nle-c[Asp^5, D-Nal(2′)^7, Lys^{10}]α-MSH (4–10)-NH_2) (26), (Rho-SHU-9119; Figure 1). To visualize hMC receptors internalization, in the present study, we have used state of art (27) TPFLSM and confocal microscopy techniques on living HEK293 cells stably transfected with the individual *h*MC receptor subtypes. TPFLSM is a powerful research tool that combines the advanced optical techniques of laser scanning microscopy with long wavelength two photon fluorescence excitation to capture high-resolution, three-dimensional images of specimens tagged with highly specific fluorophores. The methodology is particularly useful to study dynamic processes in living cells and tissues, without inflicting significant, and often lethal, damage to the specimen. TPFLSM has several advantages over the traditional confocal scanning laser or conventional epifluorescence microscopy. First, this technique obviates the need for a confocal aperture to enhance the signal to noise ratio, as the probability of two-photon excitation falls off as the fourth power of distance from the focal plane. In addition, as near infrared excitation wavelengths are used for excitation, out-of-plane photobleaching of the fluorophore is highly reduced, and the exciting light can penetrate deeper into the cell than visible or UV light (27).

We also investigated the mechanism for internalization of the four *h*MCRs in HEK293 cells transiently co-expressing the individual *h*MCR subtypes and green fluorescent protein-β-arrestin fusion proteins (β-arrestin-GFP). In addition, internalization and signaling were also examined by overexpression of dynamin and dominant negative K44A dynamin with a chimeric protein composed of green fluorescent protein and β-arrestins (28–30) and *h*MCRs. Finally, acid-resistant radioligand-binding assays were performed in the absence and presence of internalization inhibitors in order to identify possible quantitative differences in the internalization mechanisms (31) of the various melanocortin receptors.

Our present data demonstrate that agonist-mediated internalization in HEK293 cells stably transfected with the four subtypes of melanocortin receptors (MC1R, MC3R, MC4R, and MC5R) follow the pathway of agonist-mediated clathrin-coated pits (29). Furthermore, imaging results show that there is no significant influence on the β-arrestin-GFP recruitment by using the second messenger-dependent protein kinase A (PKA) activator (forskolin) and the inhibitor H-89.

Experimental Section

Synthesis of labeled Rho-MTII, Rho-SHU-911

Peptides were synthesized by the solid-phase peptide synthesis (SPPS) method (25,26,32,33). To obtain the fluorescent peptide conjugates, a rhodamine derivative [mixed tetramethylrhodamine-5-(and-6)-isothiocyaate [5(6)-TRITC] isomers; Molecular Probes, Eugene, OR, USA], was coupled to the N-terminus of the peptides through a 6-aminohexanoic acid linker.

N^{α}-Fmoc-amino acids were obtained from Bachem (Torrance, CA, USA), NovaBiochem (Switzerland), and Advanced ChemTech (Louisville, KY, USA). The side chain-protecting groups were Boc, *t*-Bu Allyl and Alloc. N^{α}-Fmoc-Asp(β-Allyl)-OH, N^{α}-Fmoc-Lys(N^{ε}-Alloc)-OH, N^{α}-Fmoc-Trp(Boc)-OH, N^{α} -Fmoc-Arg(Boc)$_2$-OH, N^{α}-Fmoc-His(Boc)-OH, and N^{α}-Fmoc-6-aminohexanoic acid were used for the synthesis. Fmoc Rink amide resin was purchased from Polymer Laboratories (Amherst, MA, USA). Organic solvents and reagents were purchased from Aldrich (Milwaukee, WI, USA) and used without further purification. All peptides were synthesized by N^{α}-Fmoc SPPS using 1,3-diisopropylcarbodiimide (DIC) and 1-hydroxybenzotriazole (HOBt) as the coupling reagents.

Rink amide resin (100 mg, 0.065 mmol/g) was placed into a 5 mL polypropylene syringe with the frit on the bottom and swollen in dichloromethane (DCM; 2 mL) for 30 min and in *N*, *N*-dimethylformamide (DMF; 2 mL) for 30 min. The Fmoc-protecting group on the Rink linker was removed by 50% piperidine in DMF. After 20 min the solution of piperidine was removed and the resin was washed with DMF (2 mL, 10 times). N^{α}-Fmoc amino acid (3 eq., 0.195 mmol) and HOBt (3 eq., 0.195 mmol) were dissolved in 700 μL of DMF and then DIC (3 eq., 0.195 mmol) was added. The coupling mixture was sucked into the syringe with the resin and shaken for 1–3 h. Coupling completion was monitored with a ninhydrin test. The coupling mixture was removed and the resin was washed with DMF (2 mL, five times). The N^{α}-Fmoc group was removed with 50% piperidine in DMF over 20 min. Each coupling and deprotection step was repeated until a linear peptide with N-terminal linker (6-aminohexanoic acid) was assembled. Cyclizations through a lactam bridge were realized by using 3 eq. of 1-hydroxy-7-aza-1H-benzotriazole (HOAT), DIC in the presence of tetrahydrofuran (THF) overnight, and changing to fresh coupling reagents every second day, for up to a week until cyclization was complete. The final wash of the resin was undergone with DMF (2 mL, five times) and DCM (2 mL, five times). The product was cleaved from the resin and the side chain-protecting groups removed with a mixture of 95% trifluoroacetic acid (TFA), 2.5% triisopropylsilane (TIPS), and 2.5% water during 1.5 h. The cleaved mixture was evaporated on a rotary evaporator. The crude

peptide was dissolved in acetic acid and purified by high-performance liquid chromatography (HPLC). For the labeling, 1 mg of pure MTII (or SHU-9119) was dissolved in 100 μL of dimethyl sulphoxide (DMSO) and added to 30 μL of 1 M $NaHCO_3$ buffer to get the pH to 8.5–9. Then 1.1 eq. of the dye rhodamine (T-490 from Molecular Probes) was dissolved in 100 μL and immediately added to the solution of the peptide, and the reaction mixture was stirred at room temperature for 1 h. Then, HPLC was run when the reaction was completed, DMSO was evaporated off and purified product by RP-HPLC (C18 bonded silica column, YMC-Pack ODS-AM 150 × 4.6 mm, S-3 mm, 120A).

Cell culture and DNA transfection

The pEGFP-N1 plasmid was obtained from CLONTECH (Palo Alto, CA, USA), FuGene 6 was from Roche Diagnostics (Indianapolis, IN, USA), and HEK293 cells were from ATCC (Manassas, VA, USA). 3-Isobutyl-1-methylxanthine (IBMX), Forskolin, Conacavalin A, and Nystatin were from Sigma (St Louis, MO, USA). All restriction enzymes were from Invitrogen (Carlsbad, CA, USA); Minimum Essential Medium (MEM), fetal bovine serum, Opti MEMI medium, and Lipofectamine were from Invitrogen. H-89 and Filipin were from Calbiochem (San Diego, CA, USA).

The cDNAs encoding the human MC1, MC3, MC4, MC5 receptors in the pcDNA3.1 mammalian expression vector were obtained from Dr I. Gantz (University of Michigan Medical Center, Ann Arbor, MI). Site-directed mutagenesis was carried out to remove the stop codon of bovine β-arrestin 1 and to introduce a unique restriction site into the cDNA. The cDNA has been subcloned into the pGFP-C1 (CloneTech, Mountain View, CA, USA) expression vector using *Xho*I and *Sal*I restriction sites. The cDNA encoding the rat β-arrestin-2-GFP were kindly provided by Dr R. J. Lefkowitz laboratory (Duke University Medical Center, Durham, NC).

For stable transfection, HEK293 cells (ATCC) were grown on a 10 cm plate in MEM with Earle's Salts (Invitrogen), supplemented with 10% (v/v) heat-inactivated fetal bovine serum, penicillin G (100 μ/mL), and streptomycin (100 μg/mL), at 37 °C, in a humidified atmosphere containing 95% air and 5% CO_2 to 80–90% confluence. The cells were transfected with (0.2 μg cDNA) using the Lipofecta-mine 2000 reagent in Opti-MEM (Invitrogen), according to the manufacturer's instructions. Stably transfected cells were selected by the addition of antibiotic (G418) 24 h after the transfection.

Transient transfections for imaging were performed in HEK293 cells which had stably expressed melanocortin receptors. Cells were grown to 90–95% confluency in a 24-well plate, and transfected with β-arrestin-1-GFP or β-arrestin-2-GFP (0.3μg each), as indicated. Six hours later cells were washed with serum-free MEM and changed to the fresh MEM-growing medium. Finally, agonist treatments were performed at 37 °C in serum-free media at a concentration of 10 nM.

Confocal and two-photon fluorescence laser scanning microscopy

To directly visualize the internalization of hMCRs, recombinant HEK293 cells were grown on 35 mm Petri dishes to 50% confluency. After removal of growing medium, rhodamine-labeled agonist Rho-MTII, or antagonist Rho-SHU-9119, was added to achieve a 10^{-8} M final concentration in MEM without serum. Two-photon laser scanning microscopy was performed using 830 nm excitation light, while for single photon imaging, 540 nm excitation light was used. Fluorescent images (*x*–*y* scan) were collected at 1-min intervals (to 30 min) and after 30 min treatment of the drug, a *Z*-scan (*x*–*z* scan) is performed.

To visualize β-arrestins translocation to the cell membrane, HEK293 cells transiently co-transfected with cDNAs encoding the *h*MCRs and β-arrestin-GFP fusion proteins were washed

with MEM without serum, and Rho-MTII or Rho-SHU-9119 were added to a final concentration of 10 nM. Confocal fluorescent microscopy was performed on a Zeiss (Cincinnati, OH, USA) LSM 510 laser scanning microscope using a Zeiss 63 × 1.4 numerical aperture water immersion lens with dual line-switching excitation (488 nm for GFP, and 544 nm for rhodamine) and emission (515–540 nm GFP, and 590–610 nm for rhodamine) filter sets.

Receptor-binding assay

Competition binding experiments were performed on whole cells. hMCRs stably transfected in HEK293 cells (34,35) were seeded on 96-well plates (50 000 cells/well), 48 h before the assay. For the assay, the medium was removed and cells were washed twice with freshly prepared MEM containing 25 mM HEPES (pH 7.4), 0.2% bovine serum albumin (BSA), 1 mM 1,10-phenanthroline, 0.5 mg/L leupeptin, 200 mg/L bacitracin. The cells were then incubated with 0.14 nM [^{125}I]-[Nle^{4}, D-Phe^{7}]-α-MSH (Perkin-Elmer Life Science, Wellesley, MA, USA, 50 000 c.p.m./well) in the presence of increasing concentrations of the unlabeled peptides for 40 min at 37 °C. The medium was subsequently removed and the cells were washed twice with the assay buffer and lysed using 500 μL 0.1 M NaOH and 500 μL 1% Triton-X-100. The radioactivity was measured in a Wallac 1470 WIZARD Gamma Counter (Perkin Elmer, Boston, MA, USA). The data were analyzed using GRAPHPAD PRISM 3.1 software (San Diego, CA, USA).

Adenylate cyclase assay

HEK293 cells transfected with *h*MCRs were grown to confluence in MEM (Gibco, Carlsbad, CA, USA) containing 10% fetal bovine serum, 100 units/mL penicillin and streptomycin, and 1 mM sodium pyruvate (35). The cells were seeded on 96-well plates 48 h before assay (50 000 cells/well). For the assay, the medium was removed and the cells were rinsed with 1 mL of MEM buffer, or with Earle's balanced salt solution (EBSS; Gibco). An aliquot (0.4 mL) of the EBSS was placed in each well along with IBMX (5 μL; 0.5 mM) for 1 min at 37 °C. Varying concentrations of melanotropins (0.1 mL) were added and the cells incubated for 3 min at 37 °C, then cells will be treated with the trypsin for 30 seconds. The reaction was stopped by aspirating the buffer by adding ice-cold Tris/EDTA buffer to each well (0.06 mL). The 96-well plates were covered and placed on ice. After dislodging the cells, the suspension was transferred to polypropylene microcentrifuge tubes, and placed in a boiling water bath for 15 min. The cell lysates were centrifuged for 2 min (6500 rpm, 5000 g), and the cAMP content was measured using the TRK 432 competitive-binding assay kit, according to the manufacturer's (Amersham, Piscataway, NJ, USA) instructions.

Acid-resistant binding assay

Stably transfected HEK293 cells were seeded into 24-well plates and grown to reach 90% confluency. The cells were washed twice with MEM without serum, and 100 μL [^{125}I]-NDP-α-MSH (100 000 c.p.m.) was added in the presence of 0.1% BSA to reduce non-specific binding. The cells were incubated at 37 °C for the indicated times, and washed with 2 × 1 mL ice-cold phosphate-buffered saline (PBS; pH = 7). In order to remove the surface-bound radioligand the cells were subsequently incubated with 500 μL acid wash solution (150 mM NaCl and 50 mM acetic acid, pH = 3) at 37 °C in a water bath (36). The acid wash solution was removed from the wells and was saved as the extracellular fraction. To obtain intracellular fraction, containing the internalized radioligand, the cells were lysed with 500 μL 0.1 NaOH and 500 μL 1% Triton-X-100 for 5 min, and the radioactivity was measured in a Wallac 1470 WIZARD Gamma Counter (Perkin Elmer).

The internalization inhibitors were added to the incubation medium together with the radioligand. The concentrations of the inhibitors were as follows: sucrose (0.45 M), concanavalin A (25 μg/mL), nystatin (50 μg/mL), and filipin (Sigma; 5 μg/mL).

Data analysis

IC_{50} and EC_{50} values represent the mean of duplicate experiments performed in triplicate. IC_{50} and EC_{50} estimates and their associated standard errors were determined by fitting the data using a nonlinear least squares analysis, with the help of GRAPHPAD PRISM 4 (Graphpad Software, San Diego, CA, USA).

Computational procedures

Molecular modeling experiments employed MACROMODEL 8.1 equipped with MAESTRO 5.0 graphical interface installed on a LINUX REDHAT 8.0 system. Peptide structures were built with standard bond lengths and angles and they were minimized using OPLS-AA force field and Polak-Ribier conjugate gradient (PRCG). Optimizations were converged to a gradient RMSD <0.05 kJ/Å mol or continued until a limit of 50 000 iterations was reached. Aqueous solution conditions were simulated using the continuum dielectric water solvent model (GB/SA) as implemented in MACROMODEL. Extended cutoff distances were defined at 8 Å for Van der Waals interactions, 20 Å for electrostatics, and 4 Å for H-bonds.

Conformational profiles of the cyclic peptides were investigated by MACROMODEL's Large Scale Low Mode (LLMOD) procedure of KolossvQry (37–40) using the energy minimization parameters as described above. A total of 10 000 search steps were performed and the conformations with energy difference of 50 kJ/mol from the global minimum were saved. The structures illustrated in Figure 2 are the lowest energy conformations of superimposed of MTII/Rho-MTII and SHU-9119/Rho-SHU-9119.

Results and Discussion

In earlier work from this laboratory (24), a two photon fluorescence laser microscopy technique (TPFLSM) was used to investigate the internalization mechanism of the *h*MCR subtypes in real time. With this technique, it is possible to obtain independent images of a cell at different depths, and thus to array the images to produce a three-dimensional cell image. TPFLSM has several advantages over confocal scanning laser microscopy or conventional epifluorescence microscopy. As the rate of a molecule absorbing two-photons simultaneously is proportional to the square of the incident intensity, the probability of two-photon excitation falls off as the fourth power of distance from the focal plane. This property of the TPFLSM obviates the need for a confocal aperture to enhance the signal to noise ratio. In addition, as TPFLSM uses longer wavelength (near infrared) light to excite the chromophore, the exciting light can penetrate deeper into cell, while out-of-focal-plane photobleaching is greatly reduced.

For these studies, a functionalized rhodamine dye [5(6)-TRITC mixed isomers] was introduced at the N-terminal of the universal melanotropin agonist for melanocortin receptors MTII (25, 41) and at the N-terminal of SHU-9119 (26,42) an antagonist for the *h*MC3R and *h*MC4R, but an agonist for the *h*MC1R and *h*MC5R. To reduce potential interactions between the dye and the pharmacophore for the melanocortin 1, 3, 4, and 5 receptors, a 6-aminohexanoic acid linker was used (Figure 1). Labeled drugs were synthesized using standard SPPS with a N^{α}-Fmoc strategy (32,33). Conformational profiles of the peptides with the dye were investigated by MACROMOD-EL's (MACROMODEL 8.1) LLMOD procedure. It was evident that the rhodamine dye was quite separated from the core pharmacophore sequence [His-D-Phe/D-Nal(2′)-Arg-Trp] of Rho-MTII and Rho-SHU-9119 (Figure 2). In addition, pharmacologic radioligand binding and functional assays (cAMP assays) were performed with the fluorescent dye-

labeled peptides in HEK293 cells stably transfected with melanocortin receptors (34,35) The IC_{50} and EC_{50} values of rhodamine-labeled MTII (Rho-MTII) and SHU-9119 (Rho-SHU-9119) were very similar to those of the unlabeled MTII and SHU-9119 (labeled MTII versus free MTII and labeled SHU-9119 versus free SHU-9119 with all subtypes of melanocortin receptors stably transfected in HEK293 cells are illustrated in Figure 3). These data indicate that the derivatization did not significantly modify the binding properties of the ligands at the *h*MCRs.

Two-photon fluorescence laser scanning microscopy imaging was performed with the labeled drugs Rho-MTII or Rho-SHU-9119 using stably transfected HEK293 cells expressing individual melanocortin receptor subtypes. In control experiments we used untransfected HEK293 cells that were not labeled with Rho-MTII, or Rho-SHU-9119 (data not shown). In additional control experiments we also demonstrated that the free rhodamine dye in itself does not interact with the melanocortin receptor expressing HEK293 cells. Conversely, in HEK293 cells stably transfected with hMC receptors, the rhodamine-labeled peptides produced a dose-dependent increase in cellular fluorescence. Fluorescent images were obtained from the ligand-treated cells at 1-min intervals for 30 min. The fluorescent-labeled agonist, Rho-MTII fully translocated into intracellular compartments within 10 min in HEK293 cells expressing *h*MCRs (Figure 4), whereas the fluorescent-labeled antagonist, Rho-SHU-9119, remained completely on the cell surface of the HEK293 cells which were stably transfected with hMC3 and hMC4 receptors, even after 30 min treatment (Figure 4). As expected Rho-SHU-9119 internalization was observed in HEK293 cells stably expressing the *h*MC1 and *h*MC5 receptors. These results provide further evidence of earlier results from our laboratory that SHU-9119 (26) behaves as an antagonist at the *h*MC3 and *h*MC4 receptors, but functions as an agonist at the *h*MC1 and *h*MC5 receptors. Our recent finding confirms these data, and illustrates the usefulness of the TPFLSM technique to determine the agonist/antagonist properties of novel ligands without requiring a detailed knowledge about intracellular signal transduction pathways. This property of the TPFLSM technique would be especially advantageous in screening putative lig-and libraries for orphan G-protein-coupled receptors (GPCR).

In order to investigate and differentiate the molecular mechanism of agonist-mediated internalization in all subtypes of *h*MCRs expressed in HEK293 cell lines (43–48) fluorescent imaging experiments were also performed in HEK cells transiently co-transfected with all subtypes of *h*MCRs and green fluorescence protein (GFP)-conjugated β-arrestins 1 and 2 (β-arrestin-1-GFP and β-arrestin-2-GFP). The confocal fluorescence imaging show that prior to agonist addition, both β-arrestin-1-GFP and β-arrestin-2-GFP, are evenly distributed throughout the cells in the case of each *h*MCR subtype (Figure 5). A parallel experiment in absence of receptors in HEK293 cells was underwent and no changes were observed (data not shown). Conversely, after addition of MTII, β-arrestin-2-GFP quickly translocated to the cell membrane for all four types of melanocortin receptors that respond to α-melanotropin (*h*MC1R, *h*MC3R, *h*MC4R, and *h*MC5R) in the stably transfected cell line (Figure 5). Similar results were obtained with a β-arrestin-1-GFP co-transfected with hMCR4 after treatment with agonist (MTII; data not shown). These observations have revealed the involvement of an agonist-mediated clathrin-dependent internalization pathway in HEK293 cells stably transfected with *h*MCRs. It is important to mention here that in our studies, we have treated the drug directly in the living cell system, instead of growing cells on dishes with coverslip inserts that may cause lowering of image resolution, and thus attain the dynamic properties of the living cell system in real time in response to the drugs.

The major mechanism of internalization of GPCRs in most mammalian cells is endocytosis via clathrin-coated vesicles (49–51). This occurs when the receptor is in an agonist-bound state, indicating that the receptor needs to be in an active conformation in order to stimulate endocytosis. In the active conformation, the majority of GPCRs are phosphorylated by G-

protein-coupled receptor kinases (GRKs; 52–54) which then leads to the binding of the cytosolic protein, *β*-arrestin. Arrestin binding physically uncouples the receptor from G proteins and recruits it into clathrin-coated microdomains in the cell membrane. The final step that completes vesicle formation is the cleavage of the budding vesicle from the cell membrane by dynamin, a 100 kDa GTPase protein. An alternative route for receptor internalization in certain mammalian cells is via the caveolae-mediated pathway. Caveolae, vesicular invaginations in the plasma membrane that contain the scaffolding protein caveolin, specific lipids, and cholesterol are morphologically distinct from clathrin-coated vesicles, but their budding and fission is also dynamin dependent (55–57). Thus, the caveolae internalization pathway can be distinguished from clathrin-mediated internalization by measuring the sensitivity of the internalization to sterol-binding agents, such as filipin and nystatin (58).

We also investigated the relative involvement of clathrin-coated pits, and caveolae-dependent internalization pathways in hMCRs internalization. In order to get quantitative data in these assays, acid-resistant radioligand binding was measured in the absence and presence of specific inhibitors of the clathrin-mediated (hypertonic sucrose, concanavalin A) and the caveolae-mediated (nystatin, filipin) pathways. Our results show that agonist-mediated internalization was significantly inhibited by hypertonic sucrose and concanavalin A at all the four subtypes of *h*MCRs (Figure 6). But that was not the case with nystatin and filipin (Figure 7). These data further confirm that agonist-mediated internalization in HEK293 cells stably transfected with *h*MCRs operate through clathrincoated vesicles, while the involvement of the caveolae pathway is minimal in this particular receptor system.

Finally, to identify whether the second messenger-dependent PKA (56,58) is involved in the agonist-mediated internalization, HEK293 cells expressing hMCRs and *β*-arrestin-2-GFP were treated with forskolin (activator of adenylate cyclase) and H89 (a PKA inhibitor). It was observed that there is no significant increase or decrease in the recruitment of *β*-arrestin-2-GFP based on the time–course (Figure 8). This observation suggests that agonist-mediated *β*-arrestin-2-GFP recruitment is not dependent on PKA activation. Similar findings were reported earlier for the adrenergic receptor (50) where it was shown that in the absence of agonist-induced conformational change of the receptor, activation of PKA by forskolin has little influence on the internalization of the receptor. The function and expression of the receptor is likely to be a major determinant for its response to agonist MTII.

The major findings of the present study can be summarized as follows: TPFLSM technique can serve as a rapid, real time screening method to differentiate between agonists and antagonists irrespective of any knowledge of their intracellular functional properties (orphan receptors). This can be achieved either through co-transfected *β*-arrestins-GFP or fluorescence-labeled ligands. In the future, TPFLSM technology can also be developed with robots for high throughput screening of combinatorial chemical libraries. This study also provides evidence that all wild subtypes of melanocortin receptors which responds to *α*-MSH (*h*MCR1, *h*MCR3, *h*MCR4, *h*MCR5) share the same mechanism of agonist-mediated internalization, i.e. all the *h*MCRs are subject to agonist-dependent endocytosis via clathrin-coated pits. This is in parallel with the observation of Gao *et al.* (43) and Shinyama *et al.* (58). who examined the MC4R by using a chimeric protein, composed of the MC4R and GFP to study MC4R localization and trafficking. Nevertheless, fusion of a large protein unit (GFP) with the receptor may significantly affect the receptor trafficking (GFP may contribute additional phosphorylation sites, trafficking motifs, etc. to the resulting chimera). Therefore, using wild type of hMCRs in this study is a marked improvement over the previous investigations where MC4R chimera was used. However, as discussed above, we went much further with our analysis/investigations of various subtypes of melanocortin receptors.

On the other hand, we have observed that β-arrestin-2-GFP recruitment is not dependent on PKA activation. Agonist-activated receptor conformation change might be critical for the β-arrestin recruitment. Furthermore, there are no significant differences between each subtype of receptor based on the time–course of internalization of the fluorescent-labeled ligand and agonist-activated β-arrestins-GFP recruitment. Further studies of desensitization and resensitization of agonist-mediated internalization using these methods will provide new additional insights into the selective mechanisms for regulation of *h*MCRs signaling. In addition, such studies can be very useful for drug discovery studies for other GPCRs.

Acknowledgements

This work is supported by grants from the U.S. Public Health Service (DK 17420 and DA 06284). We sincerely thank Professor Robert Lefkowitz and Professor Ira Gantz for the cDNA probes. The opinions expressed in this manuscript are those of the authors and no necessarily those of the USPHS.

References

1. Cone, RD. The Melanocortin Receptors. Totowa, New Jersey: Humana Press; 2000.
2. Starowicz K, Przewlocka B. The role of melanocortins and their receptors in inflammatory processes, nerve regeneration and nociception. Life Sci 2003;73:823–847. [PubMed: 12798410]
3. Mountjoy KG, Robbins LS, Mortrud MT, Cone RD. The cloning of a family of genes that encode the melanocortin receptors. Science 1992;257:1248–1251. [PubMed: 1325670]
4. Xia Y, Skoog V, Muceniece R, Chhajlani V, Wikberg JE. Polyclonal antibodies against human melanocortin MC1 receptor: preliminary immunohistochemical localisation of melanocortin MC1 receptor to malignant melanoma cells. Eur J Pharmacol 1995;288:277–283. [PubMed: 7774671]
5. Li SJ, Varga K, Archer P, Hruby VJ, Sharma SD, Kesterson RA, Cone RD, Kunos G. Melanocortin antagonists define two distinct pathways of cardiovascular control by α- and γ-melanocyte-stimulating hormones. Neuroscience 1996;16:5182–5188. [PubMed: 8756446]
6. Hagan MM, Rushing PA, Schwartz MW, Yagaloff KA, Burn P, Woods SC. Role of the CNS melanocortin system in the response to overfeeding. J Neurol Sci 1999;19:2362–2367.
7. Cone RD. The central melanocortin system and its role in energy homeostasis. Ann Endocrinol 1999;60:3–9.
8. Tritos NA, Maratos-Flier E. Two important systems in energy homeostasis: melanocortins and melanin-concentrating hormone. Neuropeptides 1999;33:339–349. [PubMed: 10657511]
9. Gantz I, Fong TM. The Melanocortin System. Am J Physiol 2003;284:E468–E474.
10. Wessells H, Fuciarelli K, Hansen J, Hadley ME, Hruby VJ, Dorr R, Levine N. Synthetic melanotropic peptide initiates erections in men with psychogenic erectile dysfunction: double-blind, placebo controlled crossover study. J Urol 1998;160:389–393. [PubMed: 9679884]
11. Van der Ploeg LHT, Martin WJ, Howard AD, Nargund RP, Austin CP, Guan X, Drisko J, et al. A role for the melanocortin 4 receptor in sexual function. Proc Natl Acad Sci U S A 2002;99:11381–11386. [PubMed: 12172010]
12. Hruby VJ, Cai M, Grieco P, Han G, Kavarana M, Trivedi D. Exploring the stereostructural requirements of peptide ligands for the melanocortin receptors. Ann N Y Acad Sci 2003;994:12–20. [PubMed: 12851293]
13. Vaudry H, Eberle AN. [^{111}In]DTPA-labeled analogs of α-MSH for the detection of MSH receptors in vitro and in vivo. The melanotropic peptides. Ann N Y Acad Sci 1993;680:1–687.
14. Hadley, ME. The Melanotropic Peptides. I–III. Boca Raton, FL: CRC Press; 1988. Source, Synthesis, Chemistry, Secretion, Circulation, and Metabolism.
15. Cone RD. The Melanocortin System. Ann N Y Acad Sci 2003;994:1–387.
16. Hughes S, Smith ME, Bailey CJ. Beta-endorphin and corticotropin immunoreactivity and specific binding in the neuromuscular system of obese-diabetic mice. Neuroscience 1992;48:463–468. [PubMed: 1318515]
17. Chhajlani V. Distribution of cDNA of melanocortin receptor subtypes in human tissues. Biochem Mol Biol Int 1996;38:73–80. [PubMed: 8932521]

18. Raffin-Sanson ML, Bertherat J. MC3 and MC4 receptors: complementary role in weight control. Eur J Endocrinol 2001;144:207–208. [PubMed: 11248737]
19. Abbott CR, Rossi M, Kim MS, Al Ahmed SH, Taylor GM, Ghatei MA, Smith DM, Bloom SR. Investigation of the melanocyte stimulating hormones on food intake. Lack of evidence to support a role for the melanocortin-3-receptor. Brain Res 2000;869:203–210. [PubMed: 10865075]
20. Chen WB, Kelly MA, Opitz Araya X, Thomas RE, Low MJ, Cone RD. Exocrine gland dysfunction in MC5-R-deficient mice: evidence for coordinated regulation of exocrine gland function by melanocortin peptides. Cell 1997;91:789–798. [PubMed: 9413988]
21. Vergoni AV, Bertolini A. Role of melanocortins in the central control of feeding. Eur J Pharmacol 2000;405:25–32. [PubMed: 11033311]
22. Chen AS, Marsh DJ, Trumbauer ME, Frazier EG, Guan X-M, Yu H, Rosenblum CI, et al. Inactivation of the mouse melanocortin-3 receptor results in increased fat mass and reduced lean body mass. Nat Genet 2000;26:97–102. [PubMed: 10973258]
23. Clark R, Knoll B, Barber R. Partial agonists and G protein-coupled receptor desensitization. Trends Pharmacol Sci 1999;20:279–286. [PubMed: 10390646]
24. Cai M, Stankova M, Pond SJK, Mayorov AV, Perry JW, Yamamura HI, Trivedi D, Hruby VJ. Real time differentiation of G-protein coupled receptor (GPCR) agonist and antagonist by two photon fluorescence laser microscopy. J Am Chem Soc 2004;26:7160–7161. [PubMed: 15186137]
25. Al-Obeidi F, Hadley ME, Pettitt BM, Hruby VJ. Design of a new class of superpotent cyclic α-melanotropins based on quenched dynamic simulations. J Am Chem Soc 1989;111:3413–3416.
26. Hruby VJ, Lu D, Sharma SD, Castrucci A, De L, Kesterson RA, Al-Obeidi FA, Hadley ME, Cone RD. Cyclic lactam α-melanotropin analogs of Ac-Nle4-cyclo[Asp5, D-Phe7, Lys10]-α-melanocyte-stimulating hormone-(4–10)-NH2 with bulky aromatic amino acids at position 7 show high antagonist potency and selectivity at specific melanocortin receptors. J Med Chem 1995;38:3454–3461. [PubMed: 7658432]
27. Xu, C.; Webb, W. Nonlinear and Two-Photon Induced Fluorescence. Lakowicz, J., editor. 5. New York: Plenum Press; 1997. p. 471-541.
28. Shenoy SK, Lefkowitz RJ. Multifaceted roles of β-arrestins in the regulation of seven-membrane-spanning receptor trafficking and signaling. Biochem J 2003;375:503–515. [PubMed: 12959637]
29. Lefkowitz RJ. G protein-coupled receptors: III. New roles for receptor kinases and β-arrestins in receptor signaling and desensitization. J Biol Chem 1998;273:18677–18680. [PubMed: 9668034]
30. Gurevich VV, Dion SB, Onorato JJ, Ptasienske J, Kim CM, Sterne-Marr M, Hosey JM, Benovic JL. Arrestin interactions with G protein-coupled receptors. Direct binding studies of wild type and mutant arrestins with rhodopsins, β2-adrenergic, and m2 muscarinic cholinergic receptors. J Biol Chem 1995;270:720–731. [PubMed: 7822302]
31. Hunyady L, Baukal AJ, Balla T, Catt KJ. Independence of type I angiotensin II receptor endocytosis from G protein coupling and signal transduction. J Biol Chem 1994;269:24798–24804. [PubMed: 7929158]
32. Hruby, VJ.; Meyer, JP. Chemical synthesis of peptides. In: Hecht, SN., editor. Bioorganic Chemistry: Peptides and Protein. New York, USA: Oxford University Press; 1998. p. 27-64.
33. Grieco P, Gitu PM, Hruby VJ. Preparation of 'side-chain-to-side-chain' cyclic peptides by allyl and alloc strategy: potential for library synthesis. J Pept Res 2001;57:250–256. [PubMed: 11298927]
34. Gantz I, Miwa H, Konda Y, Shimoto Y, Tashiro T, Watson SJ, Delvalle J, Yamada T. Molecular cloning, expression, and gene localization of a fourth melanocortin receptor. J Biol Chem 1993;268:15174–15179. [PubMed: 8392067]
35. Cai M, Mayorov AV, Cabello C, Stankova M, Trivedi D, Hruby VJ. Novel 3D pharmacophore of α-MSH/γ-MSH hybrids leads to selective human MC1R and MC3R analogues. J Med Chem 2005;48:1839–1848. [PubMed: 15771429]
36. Baig AH, Swords FM, Szaszak J, King PJ, Hunyady L, Clark AJL. Agonist activated adrenocorticotropin receptor internalizes via a clathrin-mediated G protein receptor kinase dependent mechanism. Endocr Res 2002;28:281–289. [PubMed: 12530627]
37. Cai M, Cai C, Mayorov AV, Xiong C, Cabello CM, Solos-honok VA, Swift JR, Trivedi D, Hruby VJ. Biological and conformational study of β-substituted prolines in MT-II template: steric effects leading to human MC5 receptor selectivity. J Pept Res 2004;63:116–131. [PubMed: 15009533]

38. KolossvQry I, Keser4 GM. Hessian-free low-mode conformational search for large-scale protein loop optimization: application to C-Jun N-terminal kinase JNK3. J Comput Chem 2001;22:21–30.
39. Parish C, Lombardi R, Sinclair K, Smith E, Goldberg A. A comparison of the Low Mode and Monte Carlo conformational search methods. J Mol Graph Model 2002;21:129–150. [PubMed: 12398344]
40. Greenidge PA, Merette SAM, Beck R, Dodson G, Goodwin CA, Scully MF, Spencer J, Weiser J, Deadman JJ. Generation of ligand conformations in continuum solvent consistent with protein active site topology: application to thrombin. J Med Chem 2003;46:1293–1305. [PubMed: 12672230]
41. Fan W, Boston BA, Kesterson RA, Hruby VJ, Cone RD. Role of melanocortinergic neurons in feeding and the agouti obesity syndrome. Nature 1997;385:165–168. [PubMed: 8990120]
42. Li SJ, Varga K, Archer P, Hruby VJ, Sharma SD, Kesterson RA, Cone RD, Kunos G. Melanocortin antagonists define two distinct pathways of cardiovascular control by α- and γ-melanocyte-stimulating hormones. J Neurosci 1996;16:5182–5188. [PubMed: 8756446]
43. Gao Z, Lei D, Welch J, Le K, Lin J, Feng S, Duhl D. Agonist-dependent internalization of the human melanocortin-4 receptors in human embryonic kidney 293 cells. J Pharm Exp Ther 2003;307:870–877.
44. Lohse M, Benovic J, Codina J, Caron M, Lefkowitz RJ. beta-Arrestin: a protein that regulates beta-adrenergic receptor function. Science 1990;248:1547–1550. [PubMed: 2163110]
45. Pierce K, Lefkowitz RJ. Classical and new roles of β-arrestins in the regulation of G-protein-coupled receptors. Nat Rev Neurosci 2001;2:727–733. [PubMed: 11584310]
46. Zhang J, Barak LS, Winkler KE, Caron MG, Ferguson SSG. A central role for beta-arrestins and clathrin-coated vesicle-mediated endocytosis in beta2-adrenergic receptor resensitization. Differential regulation of receptor resensitization in two distinct cell types. J Biol Chem 1997;272:27005–27014. [PubMed: 9341139]
47. Oakley RH, Laporte SA, Holt JA, Barak LS, Caron MG. Association of beta-arrestin with G protein-coupled receptors during clathrin-mediated endocytosis dictates the profile of receptor resensitization. J Biol Chem 1999;274:32248–32257. [PubMed: 10542263]
48. Tsao PI, von Zastrow M. Diversity and specificity in the regulated endocytic membrane trafficking of G-protein-coupled receptors. Pharmacol Ther 2001;89:139–147. [PubMed: 11316517]
49. Claing A, Laporte SA, Caron MG, Lefkowitz RJ. Endocytosis of G protein-coupled receptors: roles of G protein-coupled receptor kinases and β-arrestin proteins. Prog Neurobiol 2002;66:61–79. [PubMed: 11900882]
50. Menard L, Ferguson SSG, Zhang J, Lin FT, Lefkowitz RJ, Caron MG, Barak LS. Synergistic regulation of β2-adrenergic receptor sequestration: intracellular complement of β-adrenergic receptor kinase and β-arrestin determine kinetics of internalization. Mol Pharmacol 1997;51:800–808. [PubMed: 9145918]
51. Krupnick JG, Santini F, Gagnon AW, Keen JH, Benovic JL. Modulation of the arrestin-clathrin interaction in cells. Characterization of β-arrestin dominant-negative mutants. J Biol Chem 1997;272:32507–32512. [PubMed: 9405462]
52. Pitcher JA, Freedman NJ, Lefkowitz RJ. G protein-coupled receptor kinases. Ann Rev Biochem 1998;67:653–692. [PubMed: 9759500]
53. Nakamura K, Krupnick JG, Benovic JL, Asoli M. Signaling and phosphorylation-impaired mutants of the rat follitropin receptor reveal an activation- and phosphorylation-independent but arrestin-dependent pathway for internalization. J Biol Chem 1998;273:24346–24354. [PubMed: 9733722]
54. Dicker F, Quitterer U, Winstel R, Honold K, Lohse MJ. Phosphorylation-independent inhibition of parathyroid hormone receptor signaling by G protein-coupled receptor kinases. Proc Natl Acad Sci U S A 1999;96:5476–5481. [PubMed: 10318908]
55. Okamoto Y, Ninomiya H, Miwa S, Masaka T. Cholesterol oxidation switches the internalization pathway of endothelin receptor type A from caveolae to clathrin-coated pits in Chinese hamster ovary cells. J Biol Chem 2000;275:6439–6446. [PubMed: 10692447]
56. Schnitzer JE, Oh P, Pinney E, Allard J. Filipin-sensitive caveolae-mediated transport in endothelium: reduced transcytosis, scavenger endocytosis, and capillary permeability of select macromolecules. J Cell Biol 1994;127:1217–1232. [PubMed: 7525606]
57. Henley JR, Krueger EW, Oswald BJ, McNiven MA. Dynamin-mediated internalization of caveolae. J Cell Biol 1998;141:85–99. [PubMed: 9531550]

58. Shinyama H, Masuzaki H, Fang H, Flier JS. Regulation of melanocortin-4 receptor signaling: agonist-mediated desensitization and internalization. Endocrinology 2003;144:1301–1314. [PubMed: 12639913]

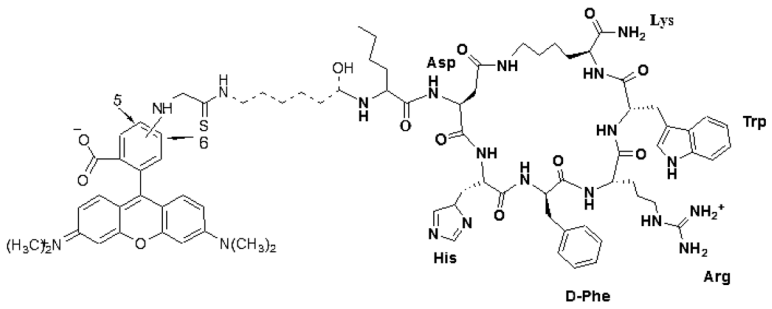

Figure 1.
Structure of super-potent agonist Rho-MTII. Bold line is MTII, dash line is linker, and regular line is rhodamine. In the case of the antagonist (SHU-9119), D-Nal (2′)[7] is substituted for D-Phe[7] in MTII.

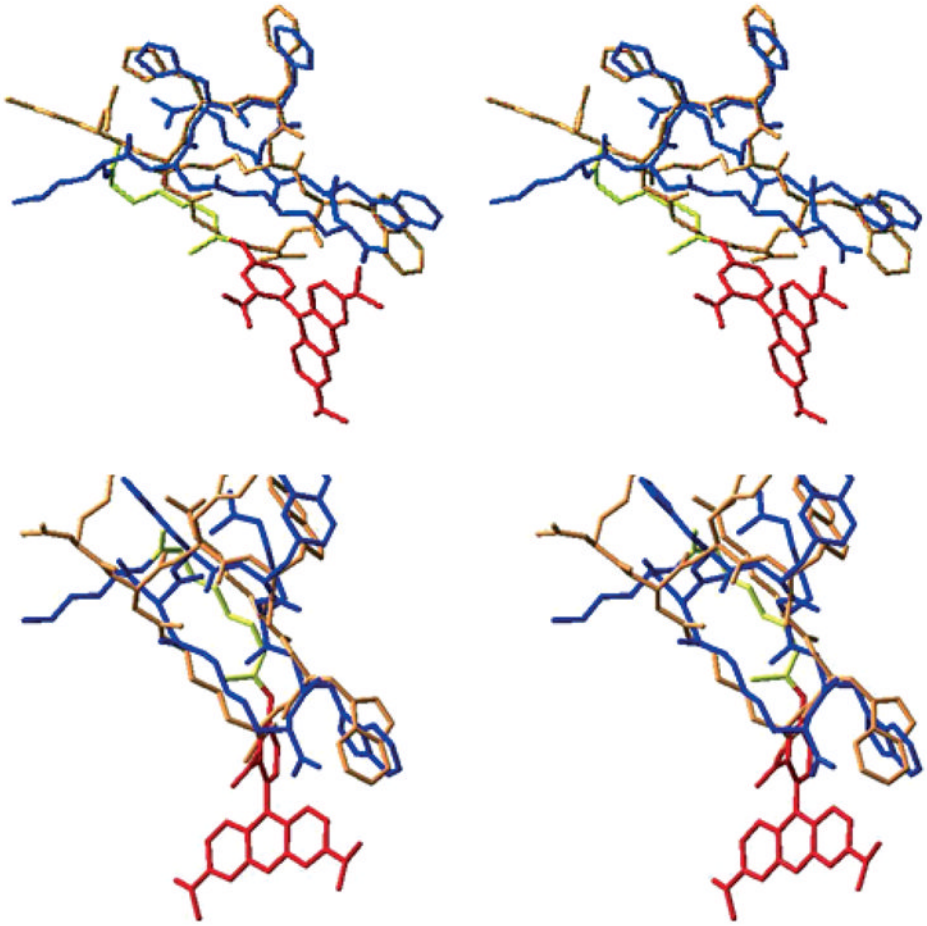

Figure 2.
Three-dimensional structure of MTII, SHU-9119, and their rhodamine-labeled derivatives. Upper: superimposed MTII (blue) and Rho-MTII (orange with yellow link and red dye) from LLMOD-derived structure. Lower: superimposed SHU-9119 (blue) and Rho-SH-U-9119 (orange with yellow link and red dye) from LLMOD-derived structure.

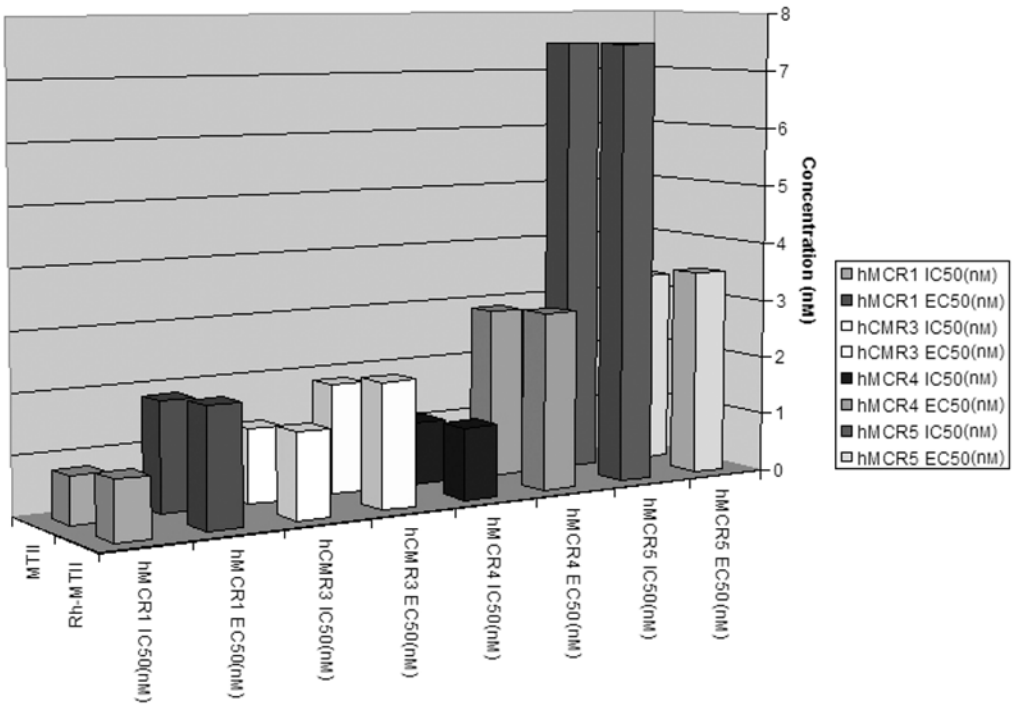

Figure 3.

Binding affinities (IC_{50}) and cAMP activities (EC_{50}) for MTII versus Rho-MTII at all subtypes of melanocortin receptors stably transfected in HEK293. There is no significant change of biologic function at each subtype of melanocortin receptors with or without the rhodamine dye.

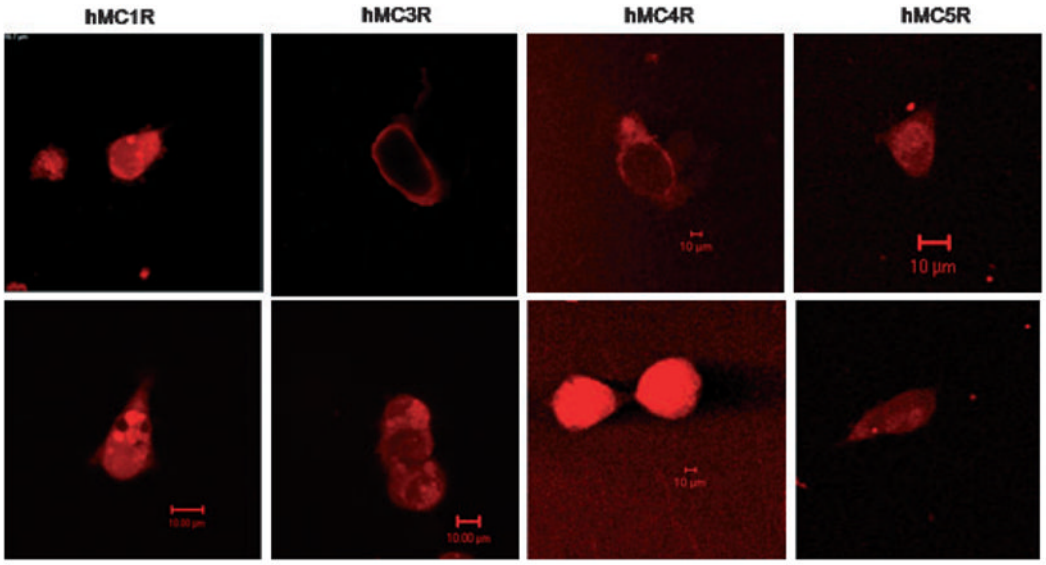

Figure 4.

Real time two-photon fluorescence laser scanning microscopy and confocal images of HEK293 cells which have of stably expressed human melanocortin receptors with its agonist (Rho-MTII), within 10 min treatment with the agonist (10 nM; lower), the agonist–receptor complex totally internalized at each subtypes of melanocortin receptors stably transfected cell lines; however, antagonist (Rho-SHU-9119; upper) even after 30 min treatment with the drug (10 nM), antagonist–receptor complex still retain on the cell surface at *h*MC3R and *h*MC4R. Laser excitation for TPFLSM was at 830 nm. The whole cell binding studies were performed at 37 °C in the presence of Minimum Essential Medium (MEM) without serum. Cells were washed two times before adding drugs.

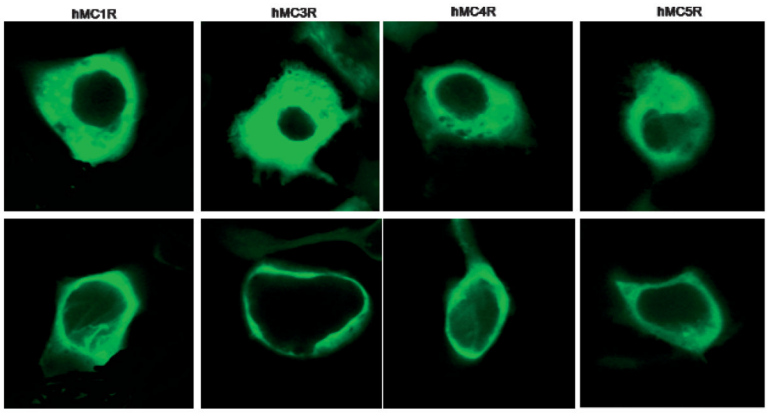

Figure 5.

Fluorescence imaging of the agonist-mediated relocalization of *β*-arrestin-2-GFP at the cell surface of HEK293 cells transiently co-transfected with *h*MCRs and *β*-arrestin-2-GFP. Upper: *β*-arrestin-2-GFP transiently transfected into HEK293 with *h*MCRs, without any treatment of the drug, *β*-arrestin-2-GFP are evenly distributed inside of the cytoplasm at each subtypes of transfected cell line; Lower: *β*-arrestin-2-GFP transiently transfected into HEK293 with *h*MCRs and treated with MTII (10 nM), after 10 min, *β*-arrestin-2-GFP relocalized to the cell membrane at each subtypes of transfected melanocortin cell lines. The whole cell imaging studies were performed at 37 °C in the presence of Minimum Essential Medium (MEM) without serum. Cells were washed two times before adding drugs.

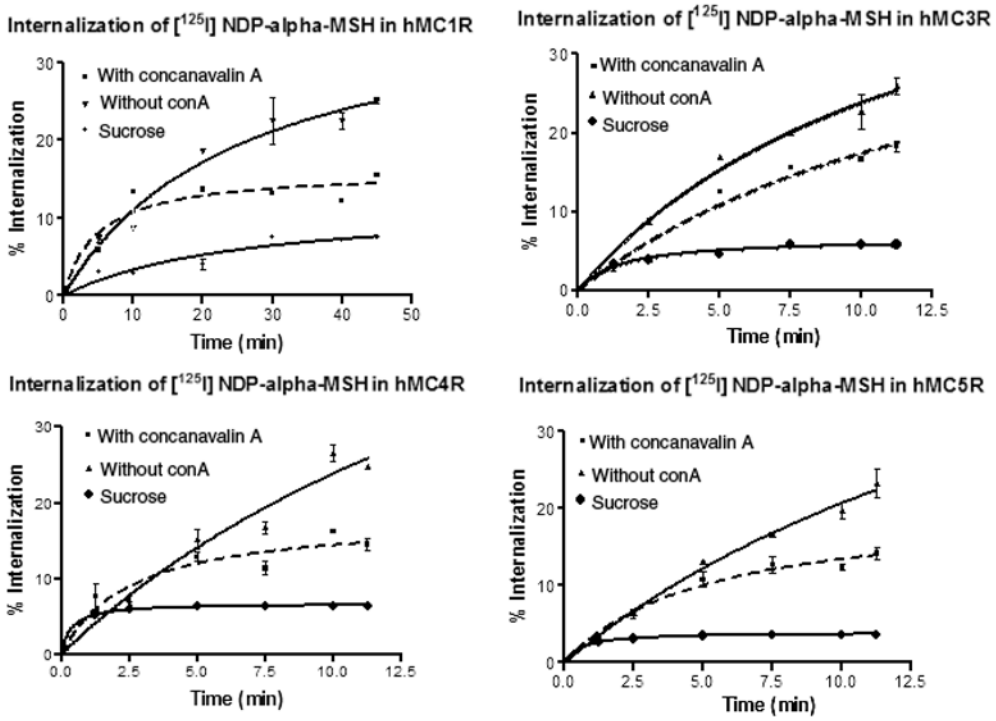

Figure 6.

Internalization of the *h*MCRs in HEK293 cells. Cells were incubated with [^{125}I]-NDP-α-MSH without treatment of concanvalin (▼); with treatment of concanavalin A (|) or with treatment of 0.4–5 M sucrose (•) at 37 °C for the indicated times. Acid-resistant and acid-sensitive binding were determined. The internalization (acid-resistant binding) was measured as a function of total binding at each time-point.

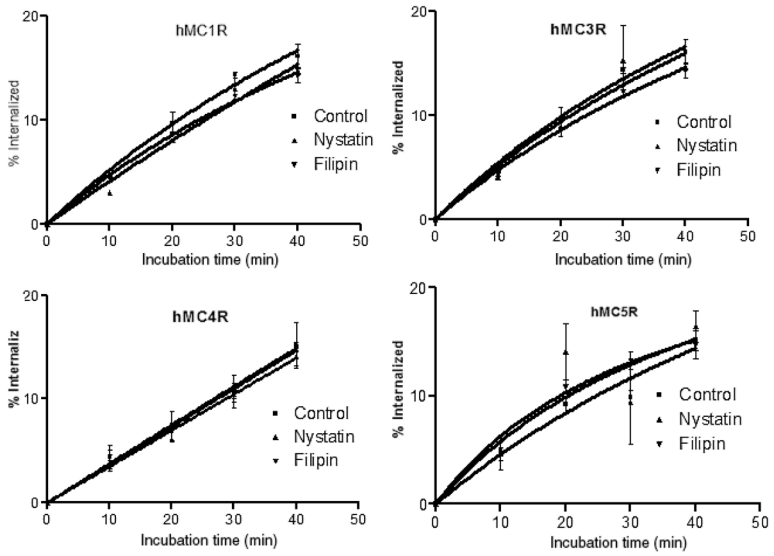

Figure 7.

Internalization of the hMCRs in HEK293 cells. Cells were incubated with [^{125}I]-NDP-α-MSH and caveolae inhibitors, filipin (▼) and nystatin (▼) compared with control (|) at 37 °C for the indicated times. Acid-resistant and acid-sensitive binding were determined. Percentage internalization (acid-resistant binding) was expressed by measuring total binding at each time-point.

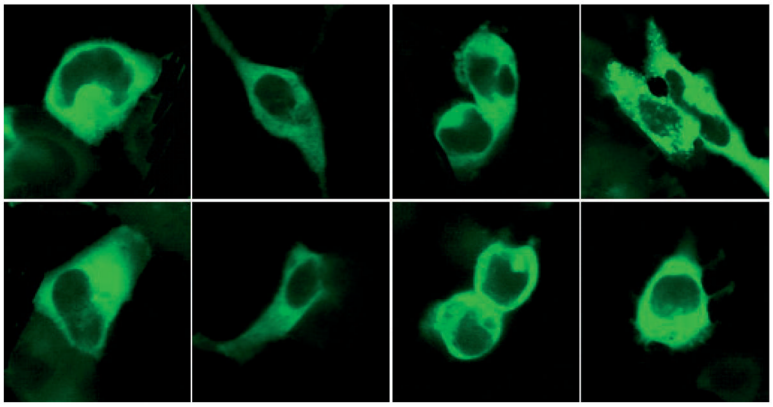

Figure 8.

Fluorescence imaging of HEK293 cells transiently co-transfected with *β*-arrestin-2-GFP and hMCRs treated with forskolin and H89. Upper: *β*-arrestin-2-GFP transiently transfected into HEK293 with hMCRs and treated with H-89 (100 nM), after 10 min. Lower: *β*-arrestin-2-GFP transiently transfected into HEK293 with hMCRs and treated with forskolin (100 nM) after 10 min. There is no significant relocalization of *β*-arrestin-2-GFP at each subtypes of the transfected cells. The whole cell imaging were performed at 37 °C. Cells were washed two times with the binding buffer before adding drugs.